

Submitted to the *Journal of Neuroscience*,
Behavioral/Systems Neuroscience Section,
Dr. Stephen G. Lisberger, Section Editor

Temporal structure in neuronal activity during working memory in Macaque parietal cortex

Bijan Pesaran¹, John Pezaris², Maneesh Sahani², Partha P. Mitra³
and Richard A. Andersen^{2,4}

¹ Division of Physics, Mathematics
and Astronomy
California Institute of Technology
Pasadena, CA 91125

² Computation and Neural
Systems Program
California Institute of Technology
Pasadena, CA 91125

³ Bell Laboratories
Lucent Technologies
Murray Hill, NJ 07974

⁴ Division of Biology
California Institute of Technology
Pasadena, CA 91125

Abbreviated Title: Temporal structure during working memory
Page Count: 41 (excluding figures)
Figure Count: 15
Table Count: 0
Word Counts: Abstract, 241; Introduction, 519; Discussion, 1550

Acknowledgments: This work was supported by NIH grant EY05522-21, ONR grant N00014-94-0412, Bell Labs, Lucent Technologies internal funding, the Keck Foundation, the Sloan Foundation, and the Workshop for the Analysis of Neural Data, MBL, Woods Hole, MA (<http://www.vis.caltech.edu/~WAND>)

Please address correspondence to:

Richard A. Andersen
Division of Biology 216-76
California Institute of Technology
Pasadena, CA 91125
andersen@vis.caltech.edu
(626) 395-8336 (Office) (626) 795-2397 (Fax)

Abstract

A number of cortical structures are reported to have elevated single unit firing rates sustained throughout the memory period of a working memory task. How the nervous system forms and maintains these memories is unknown but reverberating neuronal network activity is thought to be important. We studied the temporal structure of single unit (SU) activity and simultaneously recorded local field potential (LFP) activity from area LIP in the inferior parietal lobe of two awake macaques during a memory-saccade task. Using multitaper techniques for spectral analysis, which play an important role in obtaining the present results, we find elevations in spectral power in a 50–90Hz (gamma) frequency band during the memory period in both SU and LFP activity. The activity is tuned to the direction of the saccade providing evidence for temporal structure that codes for movement plans during working memory. We also find SU and LFP activity are coherent during the memory period in the 50–90Hz gamma band and no consistent relation is present during simple fixation. Finally, we find organized LFP activity in a 15–25Hz frequency band that may be related to movement execution and preparatory aspects of the task. Neuronal activity could be used to control a neural prosthesis but SU activity can be hard to isolate with cortical implants. As the LFP is easier to acquire than SU activity, our finding of rich temporal structure in LFP activity related to movement planning and execution may accelerate the development of this medical application.

Keywords: parietal, prosthesis, local field potential, gamma band, coherence, temporal structure.

Working memory is a brain system requiring the temporary storage and manipulation of information necessary for the performance of complex cognitive tasks (Baddeley, 1992). The neurophysiological basis of working memory is studied in non-human primates by recording neural activity during delayed-response tasks (Fuster, 1995). Cue-selective elevated single unit firing rates have been recorded during the delay period in many brain areas during different versions of the task (Fuster and Jervey, 1982; Bruce and Goldberg, 1985; Gnadt and Andersen, 1988; Miyashita and Chang, 1988; Funahashi et al., 1989; Koch and Fuster, 1989; Miller et al., 1996; Zhou and Fuster, 1996). How this neural activity is sustained is unknown but may be important to understanding the neural basis of working memory (Goldman-Rakic, 1995). Converging evidence points to the importance of a distributed recurrent neuronal network (Goldman-Rakic, 1988) and reverberating network activity has long been suggested as a possible mechanism for short-term memory (Lorente de No, 1938; Hebb, 1949; Amit, 1995; Seung, 1996; Wang, 1999).

Measures with the potential to capture correlated neural activity on a millisecond time scale may be needed to resolve reverberating memory activity. The dynamical structure of neuronal activity has been the source of much interest as a temporal code (for a review see Singer and Gray (1995)) however much of this work emphasizes stimulus-induced activity and its relation to perception (Eckhorn et al., 1988; Gray et al., 1989; Engel et al., 1990; deCharms and Merzenich, 1996; Borst and Theunissen, 1999). Other work in somatosensory and motor areas reports temporal structure in activity during a period before action (Sanes and Donoghue, 1993; Bressler et al., 1993; Murthy and Fetz, 1996a; Murthy and Fetz, 1996b; Roelfsema et al., 1997) and electroencephalography (EEG) studies in humans report sustained oscillatory responses during working memory (Tallon-Baudry et al., 1999).

Elevated single unit (SU) activity in parietal cortex during a memory-saccade task was first reported on the lateral bank of the intraparietal sulcus (area LIP) (Gnadt and Andersen, 1988) and this area has now been implicated in a variety of cognitive processes (for a review

see Andersen (1995)). More recent work reports similar memory activity in parietal cortex before reaches (Snyder *et al.*, 1997) and grasps (Sakata *et al.*, 1995) relating parietal cortex to movement plans in general. There is great interest in helping paralyzed patients by using cortical SU activity to control a prosthesis (Kennedy and Bakay, 1998; Chapin *et al.*, 1999) and the relation of parietal SU activity to movement planning makes it a potentially useful signal (Shenoy *et al.*, 1999). However, the difficulty of isolating SU activity with cortical implants has presented a major hurdle to the development of a neural prosthesis. The local field potential (LFP), which measures activity in a population of neurons, is easier to acquire than SU activity. Consequently the presence of temporal structure in LFP activity could prove important for the development of this application.

We recorded SU and LFP activity from two macaques during a memory-saccade task using a single tetrode located in area LIP. SU activity has been previously examined in area LIP during this task (Gnadt and Andersen, 1988; Chafee and Goldman-Rakic, 1998) and previous analysis of this data has investigated SU activity for temporal structure. (Pezaris *et al.*, 1997b) looked for oscillations using autocorrelation functions but averaged over long periods of time and reported their absence. (Pezaris *et al.*, 1999) showed evidence for structure in auto- and cross-covariations between spike trains without examining significance. LFP activity in parietal cortex has not been previously examined. In this work, we use modern techniques of multitaper spectral analysis to investigate temporal structure in SU and LFP activity. We find significant structure in the spectrum of SU and LFP activity and the coherency between them. We also find additional significant spectral structure in LFP activity that codes for movement execution and preparatory aspects of the task. These results provide evidence for memory fields of temporal structure (dynamical memory fields) that may reflect the columnar organization of cortex.

MATERIALS AND METHODS

Animal preparation

Recordings were made from two adult male Rhesus monkeys (*Macaca mulatta*). Animals were fitted with a stainless steel head post embedded in a dental acrylic head cap to fix their head position, a scleral search coil to record eye position and a stainless steel recording chamber was placed over a craniotomy to gain access to the cortex. All surgical procedures and animal care protocols were approved by the California Institute of Technology Institutional Animal Care and Use Committee and were in accordance with National Institutes of Health Guidelines.

Behavioral task

Recordings were made while animals performed memory-saccade task (see Fig. 1). Each trial of this task begins with the illumination of a central fixation light, to which the animal saccaded. As long as the fixation light was present, the animal was required to maintain fixation within a 2° circular window. After a post-foveation background period of 1 – 2 seconds, a target light was flashed for $100ms$ at one of 8 fixed stimulus locations evenly distributed on a 10° circle. Following the target flash, the monkey had to maintain fixation for a further period of $1000ms$, at the end of which, the fixation light was extinguished, and the animal required to saccade to the remembered location of the flashed stimulus. For accurate saccades, the target was reilluminated for a minimum of $500ms$, often triggering a corrective saccade, and the animal required to fixate at the new location while the target remained on. At the completion of a successful trial, the animal was rewarded with a drop of water or juice. Target locations were randomly interleaved to collect between 10 – 15 successful trials for each location in blocked fashion.

Electrophysiological recordings

Electrical activity was recorded from the behaving monkey using single tetrodes (Reece and O'Keefe, 1989) adapted for use in the awake monkey preparation (Pezaris et al., 1997b). This is extensively described elsewhere (Pezaris, 2000), and is briefly summarized here. Tetrodes were placed in a fine guide tube and positioned using a standard hydraulic microdrive (Fred Haer Corp, Brunswick, ME). Neural signals were amplified by a custom four-channel headstage amplifier ($A = 100$, feeding a custom four-channel variable-gain preamplifier ($A = 1 - 5000$, nominally set to 200, (Pezaris, 2000)) and anti-alias filters (9-pole elliptical low-pass, $f_c = 10$ kHz, Tucker-Davis Technologies (TDT), Gainesville, FL) before being digitized with a four-channel instrumentation-grade 16-bit analog to digital converter ($f_s = 20$ kHz, also TDT). Digital data were then streamed to disk and written to CD-ROM. The polarity of the LFP was reversed to give positive-going spike activity. Continuous extracellular traces were processed off-line to extract and classify spike events and calculate the LFP. Figure 2 presents the extracellular potential from a channel of the tetrode. Panel a) presents activity during one trial and panel b) presents activity during the memory period on an expanded time base.

Spike Sorting

SU activity was extracted from the digitized recordings by an automated procedure which identified and sorted spike waveforms into clusters, each presumed to arise from a single cell. The algorithm has been motivated and described by Sahani et al. (1998) and in detail by Sahani (1999) and will be summarized here.

Prior to spike sorting, the recordings were bandpass filtered (0.6 - 6 kHz). A statistical model describing the distribution of spike shapes was then fit to waveforms extracted from 30s of data, as described below. This model was used to classify spike events in the rest of the recording.

First, candidate spike times were identified by comparing the signal to a threshold of 3 times the root-mean-square (RMS) signal value on each channel. Spikes were accepted when the trace i) crossed and remained above the threshold for at least 0.1ms on at least one channel; ii) crossed the threshold on the other channels either within 0.1ms of this time, or else not within 1ms; iii) did not remain above threshold for longer than 1ms; and iv) did not cross the threshold again within 1ms. These constraints reduced the number of overlapped spike events in order to reduce bias in estimating the spike waveform model.

A 2.4ms segment (48 samples per channel) of data was then extracted from all four channels, centered on each identified spike time. A $(2 \cdot \text{RMS})$ thresholded center of mass was calculated for each spike waveform, and the segment resampled by interpolation to yield 24 samples per channel (1.2ms), with the center of mass falling one-quarter of the way into the waveform. The precision of this center of mass alignment was 4-8 times the original sampling frequency. The different channels were then concatenated to yield 96-dimensional event vectors.

The background noise covariance expected in these event vectors was estimated using 1.2ms segments extracted from the recording at times when no threshold-crossing was seen. The event vectors were then transformed to lie in a space where this noise covariance was whitened, and a mixture of a single Gaussian and a uniform density fit to them. The principal eigenvectors of the covariance of the Gaussian provided robust estimates of the principal components of the data in the noise-whitened space. Low-dimensional event vectors were obtained by projecting each transformed event onto the four leading eigenvectors of the Gaussian covariance.

Events were clustered by fitting a mixture of Gaussian distributions to the low-dimensional event vectors. The covariance of each Gaussian was fixed at the identity matrix (since the background noise is white in the transformed event space). A uniform component was introduced in the mixture to reduce the effect of outliers. The fit was performed using the

Relaxation Expectation-Maximization algorithm (Sahani, 1999; see also Ueda and Nakano 1994) which helped to avoid problems of local minima. The correct number of Gaussian components was determined by cascading model selection (Sahani, 1999).

Each Gaussian component in the mixture was taken to represent the distribution of spikes expected from a single cell, and events were assigned to cells according to a maximum *a posteriori* rule. The autocorrelogram of spikes assigned to each cluster was checked to ensure that no violations of the refractory period were seen. To ensure that the clustering was robustly determined, the segment of data used to fit the model was varied and only models that were consistent for all segments were included in database.

Data analysis

The data are SU activity (a point process) and the LFP (a continuous valued time series) making this a hybrid data set. Spectral analysis provides a unified framework for the characterization of hybrid processes and we use multitaper methods of spectral estimation developed in Thomson (1982) to construct estimators for all spectral quantities (see **Appendix**). These estimates are presented and evaluated in (Percival and Walden, 1993) and are applied to a wide range of neurobiological data in (Mitra and Pesaran, 1999). Correlation function measures such as the auto- and cross-correlation function characterize the same statistical structure in time series as spectra and cross-spectra, however, as we discuss in a later section, spectral estimates offer significant advantages over their time domain counterparts.

Spike events were binned at 1ms time resolution to give spike trains. LFP time series were calculated from the extracellular recordings from one tetrode channel by lowpass filtering the signal at 200Hz using multitaper projection filters (Thomson, 1994). The out-of-band suppression properties of these filters ensured minimal corruption of the LFP estimate by SU activity. Controls, described below, were performed that confirm this.

MEAN RESPONSES: The mean response of SU activity, the peri-stimulus time histogram (PSTH), was calculated by counting the number of spikes per 1ms bin and averaging across trials for each saccade direction aligned to the initial target onset, followed by smoothing with a gaussian kernel, ($\sigma = 10ms$). The mean response of the LFP was calculated analogously to SU mean responses by averaging across trials for each saccade direction aligned to the initial target onset and smoothing with a gaussian kernel, ($\sigma = 10ms$). Trials were aligned to the saccade before averaging with no qualitative change in the results.

SPECTRAL ANALYSIS: Details of the multitaper techniques used to estimate the spectral quantities are presented in the **Appendix**. In brief, spectral analysis is the study of time series in the frequency domain. The frequency domain is preferred over the time domain for multiple reasons, an essential one being that neighboring points in time are usually highly correlated while neighboring points in frequency are more nearly independent. Multitaper methods for spectral estimation use special data tapers. A segment of data is multiplied by a data taper before Fourier transformation. called prolate spheroidal functions (also known as Slepian functions) that are maximally concentrated in a bandwidth in frequency, W , for a specified duration in time, T (Slepian and Pollack, 1961). In addition to being maximally concentrated in frequency and time, there are many Slepian functions for a given choice of T and W , and they are orthogonal to each other. Specifically, there are K functions that are concentrated where $K = 2p - 1$, and $p = TW$, the time-bandwidth product. The use of multiple Slepian functions as data tapers give multitaper estimates their minimum bias and variance properties.

Three periods during the trial were investigated: *baseline*, *memory* and *perisaccadic*. The baseline period was defined as extending 750ms to 250ms before the initial target onset. The memory period was defined as extending 450ms to 950ms following the initial target onset. The perisaccadic period was defined as extending from 250ms before the saccade to 250ms after the saccade. Baseline activity was estimated by pooling activity

from all successful trials. Memory and peri-saccadic activity were estimated by pooling activity from successful trials according to saccade direction.

Two saccade directions of interest were defined for SU and LFP activity, *preferred* and *anti-preferred*. The preferred direction was the direction that elicited the maximum firing rate during the period from the initial target onset to the offset of the fixation light. The anti-preferred direction was defined as the opposite direction to the preferred direction. In this study, there were no cases of multiple SUs recorded at the same site with different preferred directions. The preferred direction of the LFP was defined to be the same as the preferred direction of simultaneously recorded SU activity. Activity from different locations was aligned to the preferred direction before estimating population average quantities.

In all cases, time-frequency representations of the activity were calculated on a 500ms window that was stepped by 100ms between estimates through the trial. The time index was aligned to the center of the analysis window. As a control, window size was varied from 200–750ms without significant change in the results. In contrast to the characterization of baseline, memory and perisaccadic activity described above, time-frequency representations presented were estimated by averaging trials aligned to the initial target onset. Trials were aligned to the saccade before averaging with no qualitative change in the results. Slepian functions with different time-bandwidth products were used to estimate SU and LFP spectra, and SU-LFP coherency that best resolved significant structure in the data.

SU AND LFP SPECTRA: The spectrum, $S(f)$, is a real quantity that is a function of frequency for a given window in time and is a measure of temporal organization. For example, if single unit activity tends to cluster in time with a typical spacing, then the spectrum will show a peak at the inverse of that spacing. The spectrum is the Fourier transform of the auto-correlation function but the use of data tapers makes estimates of the spectrum less susceptible to bias and variance problems compared to the auto-correlation function.

SU spectrum was estimated on a 500ms window using 9 Slepian data tapers with time-bandwidth product, $2p = 10$ giving a frequency resolution of $\pm 10\text{Hz}$. The spectrum of SU activity estimated for each cell giving the *single cell* estimate. SU activity from each cell was aligned according to preferred direction and averaged for each saccade direction across all cells in each monkey to give the *population average*. SU spectrum significance levels were estimated with multitaper methods using the jackknife method (Thomson and Chave, 1991).

The LFP spectrum was estimated on a 500ms window using 5 Slepian data tapers with time-bandwidth product, $2p = 6$ giving a frequency resolution of $\pm 6\text{Hz}$. The spectrum of LFP activity was estimated for each recording giving the *single site* estimate. LFP activity from each site was aligned according to preferred direction and averaged for each saccade direction across all sites in each monkey to give the *population average*. LFP spectrum significance levels were estimated with multitaper methods using the jackknife method.

COHERENCY: The coherency, $C(f)$, is a complex quantity that is a function of frequency for a given window in time and measures the degree of predictability of one process using a linear function of the other (Brillinger, 1975; Rosenberg et al., 1989). Here we use a hybrid version of the coherency for point process and ordinary time series data to measure the relation between SU and LFP activity.

The magnitude of the coherency lies between zero and one and is called the coherence. Coherence indicates the strength of the relationship between the processes. The coherency is used in preference to the cross-correlation function which is usually estimated to measure the relation between two processes. In particular, increases in coherence are not due to changes in firing rates as the coherency is explicitly normalized by the spectrum of the individual processes. This is not true for the cross-correlation function which may be normalized in an *ad-hoc* fashion, but is not normalized by simple means.

SU-LFP coherency was estimated on a 500ms window using 19 Slepian data tapers with

time-bandwidth product, $2p = 20$ giving a frequency resolution of $\pm 20\text{Hz}$. The coherency of SU and LFP activity was estimated for each cell giving the *single cell* estimate. SU-LFP coherency estimates were aligned according to preferred direction and the complex coherency values averaged to give the *population coherency*. SU-LFP coherency significance levels were estimated with multitaper methods using the jackknife method.

SPIKE-TRIGGERED POTENTIAL: The relation between single unit activity and the extracellular potential was assessed with the use of a spike-triggered average of the raw data during the baseline period and memory period prior to a saccade in the preferred direction for that cell. 200ms segments of the potential centered on the SU event time were extracted. Spike waveforms were suppressed by subtracting a 2ms mean spike shape waveform. The traces were then averaged to give the spike-triggered potential. The spike-triggered potential provided a measure of association between SU activity and the extracellular potential and provided a control against corruptions in the LFP that might result from incompletely filtering out SU spike activity. 95% confidence intervals were calculated by estimating the standard error of the mean.

PHASE HISTOGRAM: The LFP was filtered between 50–90Hz using projection filters (Thomson, 1994) to give a complex valued signal. The frequency band was selected according to results of the coherency analysis. The phase of this signal was sampled at spike event times during the baseline and memory periods. Phases were pooled from the preferred direction during the memory period, and from all trial conditions during the baseline. The phases were then pooled across all cells in the study. These phases are the frequency domain version of the spike-triggered potential. The histogram of phases between the baseline and memory periods provided a control for the coherency estimate as estimation of the histograms was not limited to small numbers of spike events from a particular cell. A one-sample Kolmogorov-Smirnov test (KS test) was used to determine significance level for deviations of the phase histogram during the memory period from a uniform distribution (Rao, 1965).

A two-sample KS test was used to determine the significance level for deviations of the phase histogram during the memory period from the baseline period.

RESULTS

The database for this study contained 16 SUs recorded at 16 sites in one monkey and activity from 24 SUs recorded at 17 sites in another monkey. Since we were primarily interested in memory period activity, a subjective evaluation was made during data collection to make recordings only when tuned memory activity was present. Subsequently, during off-line analysis, recordings were further selected for containing at least one clearly and stably isolated cell, using criteria described in the **Methods** section above.

Mean SU and LFP responses

Mean SU activity in area LIP during memory-guided saccades has been characterized in previous reports (Gnadt and Andersen, 1988; Barash et al., 1991). Our results agreed with those reports and we found 28 of 40 neurons (70%) had significant memory period activity ($p < 0.05$). Figure 3 shows the response of a typical cell with memory activity. The eight trial conditions are displayed in a spatial map with eye position and behavioral events shown beneath the PSTH and spike rasters from each trial shown above. The preferred direction of this cell is for saccades to the left. Activity from this SU is presented as a running example of SU activity in subsequent single cell figures below.

Figure 4 a) shows the PSTH for a single unit across trial conditions in a 2d plot. Line plots of the spike rate in the preferred and anti-preferred directions are shown in panel b). Figure 4 c) shows the mean LFP response for a single site across trial directions and panel d) shows line plots in the preferred and anti-preferred directions. The increase of the LFP with narrow tuning during and following the initial target illumination is similar to SU activity. However, the broad, tuning of the LFP across saccade directions peri- and post-

saccadically is not observed in SU activity. This feature is a result of the increase in the mean LFP response occurring with a systematic increase in latency across trial conditions. Following the saccade, there is also a suppression in the mean LFP response that is narrowly tuned. These features are seen in recordings from all sites recorded from in area LIP in both monkeys. LFP activity recorded from this site is presented as a running example of LFP activity in subsequent single site figures below.

Temporal structure in SU and LFP activity during working memory

The maintenance of sustained memory activity may be due to the intrinsic dynamics of local or long-range networks (Hebb, 1949). These dynamics may not be revealed by a study of elevated mean firing rates or mean responses as they could involve the temporal organization of neuronal activity. Here we use multitaper techniques for spectral analysis to study the temporal structure of SU and LFP activity.

Figure 5 shows spectrograms and individual spectra of SU activity in the preferred direction for a single cell and the population average from one monkey. Panel a) shows the spectrum of SU activity during the memory (red) and baseline (blue) periods from a typical single unit in the solid line. The high-frequency limit of the spectrum in each case is shown by the horizontal dotted line. The spectrum of a poisson process with the same firing rate would fall on this line, therefore deviations of the spectrum from this line are evidence of temporal structure in SU activity. 95% error bars are shown by thin dashed lines in each case. Two significant features are present in the memory period spectrum that are absent from the baseline period. This indicates the presence of temporal structure during working memory. The first significant feature is a suppression in power at frequencies below 20Hz. The second is a peak in power at a higher frequency band, in this case centered at 50Hz. Panel b) shows a single unit spectrogram for the same unit shown in panel a). The spectrogram presents the spectrum as a function of time and the spectral structure is

sustained throughout the memory period, beginning at the initial target illumination and continuing through the saccade.

Panels c) and d) of Figure 5 show the spectrum and spectrogram for the population average. The significant features of suppression of power at low frequencies and the elevation in the gamma band during the memory period are also present and are sustained throughout the trial across a population of single units. Of the 40 single units recorded for this study, memory period activity from 21 neurons (53%) showed significant spectral peaks ($p < 0.05$) and 22 neurons (56%) showed significant spectral suppression ($p < 0.05$). In all cases, SUs that showed significant spectral structure had elevated mean firing rates during the memory period compared to the baseline period. Inspection of the individual spectra reveals that spectral suppression out to 20Hz is present across the population while the peak frequency exhibits more variability and can occur at frequencies as low as 25Hz and as high as 70Hz. Structure in SU memory period activity during saccades to the anti-preferred direction is difficult to resolve because of low spike number but, similar to baseline activity, we find no significant features in the spectrum.

If temporal structure in spiking activity is part of a neural code, it may be reflected in LFP activity. Figures 6 and 7 present results of spectral analysis of LFP activity.

Figure 6 shows line plots for activity at a single site and across a population in one monkey. Panel a) shows the power during the memory period (solid) compared to the baseline period (dotted) at a single site for trials to the preferred direction. Memory period LFP activity shows a peak similar to the SU activity. Since the LFP is a continuous time series, a study of activity for other trial conditions with lower firing rates is possible without a loss of resolution. Panel c) shows the elevated gamma band power is absent during the memory period in the anti-preferred direction (dotted). Panels b) and d) show the same information for a population average in one monkey. The gamma band peak is broader in the population average and distinct from temporal structure at lower frequencies below

25Hz. Inspection of the individual spectra reveals that this broadening is due to variability in the peak frequency at different sites in area LIP.

Figure 7 shows spectrograms for the activity presented in figure 6. Panel a) shows the spectrogram for activity at a single site during trials in the preferred direction and panel c) shows the population average. The increase in power during the memory period in a $70 \pm 20\text{Hz}$ gamma band is sustained throughout the memory period. Panels b) and d) present activity in the anti-preferred direction for single site and a population average. In both cases there is no increase of activity during the memory period. Low frequency ($20 \pm 5\text{Hz}$) beta band activity shows some organization with respect to the trial in these plots. This is presented in figure 15. The analysis of activity from a second monkey gives similar results.

Coherency between SU and LFP activity during working memory

If working memory is a network phenomenon temporal structure in SU and LFP activity may be coherent during the memory period. We investigated this possibility by calculating the coherency between SU and LFP activity.

Figure 8 shows the coherency between a single cell and the simultaneously recorded LFP averaged across all trials to the preferred direction. A sharp increase in the coherence between SU activity and the LFP can be seen at $70 \pm 20\text{Hz}$ that exceeds 99% confidence intervals. This increase is sustained through the memory period. When the coherence is significant the phase of the coherency is also well-organized in this band and has a value of zero radians. This is evidence for phase-locking between the SU and the LFP during working memory that is sustained throughout the period. In particular, the phase of the coherency indicates that during working memory the SU fires at the peak of broad-band 50 – 90Hz LFP activity. In a given window, the phase of the coherency is relatively constant across frequency indicating that SU and LFP gamma band activity are synchronous with

no time lag between them. It is important to note that since the power in each process is explicitly normalized for, the increase in coherence during the memory period is not related to power increases in either process. Instead it is a result of an increase in the predictability of one process given the other indicating that one can predict when the SU will fire from LFP activity more accurately during working memory than during simple fixation.

This result is typical of a population of cells with memory activity recorded from area LIP in two monkeys. Of the 40 single units recorded at 33 sites in this study, 18 (45%) showed significant coherence during the memory period in the $70 \pm 20\text{Hz}$ frequency band ($p < 0.01$). All single units with significant coherence with the LFP contained significant temporal structure during the memory period. A comparison of activity between multiple single units and the LFP recorded at the same site was not possible in this study as there were only two pairs of simultaneously recorded single units with significant memory period activity.

Since the coherency is well-normalized, the coherency from different recordings can be averaged to determine the population coherency. Figure 9 shows the population coherency for one monkey. The increase in coherence between the LFP and a simultaneously recorded SU is significant ($p < 0.01$) across a population average, even though the phase at different locations could be random which would reduce the population average. Activity from the second monkey shows the same results. The significant population coherency during the memory period is further evidence for locking of SU activity to temporal structure in the LFP that is activated by a working memory task. Moreover this locking occurs with the same preferred phase in all recordings from area LIP in this study.

The LFP is measured by low-pass filtering the extracellular potential recorded on the tetrode. Since the extracellular potential also contains spike events there is the possibility that the estimated coherency is a result of spectral leakage in which low frequencies present in the spikes contaminate the LFP estimate. To control for this, we suppressed spike energy

in the extracellular potential by smoothly subtracting a mean waveform at each spike event time. We then low-pass filtered the resulting signal as before and repeated the analysis. The estimated coherency was still significant.

We also performed a second control for possible contamination of the LFP estimate by SU spike events. The mean potential in a 200ms window was calculated conditional on SU spike event times for all events during the memory period and compared against those during the baseline. Figure 10 panel a) shows the spike-triggered average potential conditional on SU activity during the baseline period and panel b) shows the average conditional on SU activity during the memory period. 95% confidence intervals are shown with dotted horizontal lines. The spike-triggered potential during the memory period shows an oscillatory component that survives the average indicating that the phase of the LFP at that frequency is coherent. The baseline activity shows little coherent structure at a high frequencies but does show significant structure immediately before a spike event. The oscillations in the spike-triggered average potential during the memory period are not significant but they do have the same frequency and phase as the coherency in figure 8. Since these error bars are constructed in the time domain they are not suitable to detect band-limited structure in the frequency-domain. We present a frequency-domain alternative to the spike-triggered potential in figure 11.

The increase in the estimated coherency during the memory period may be misleading because the low number of SU spike events during the baseline period makes the estimate of coherency in that period unreliable. We performed a second control to see if the coherency between SU and LFP activity could be observed in a way that was not sensitive to small numbers of SU spike events during the baseline period. We subtracted mean spike waveforms from the raw data and bandpass filtered the raw signal at 50 – 90Hz using projection filters. The bandpassed signal is a complex number with amplitude and phase and we sampled the phase of this signal at the spike event times. Since the phase of LFP activity at SU spike

event times is normalized we can compare the coherency of activity across recordings. We pooled activity from all single units recorded in both monkeys and compared the distribution of the phase of the LFP at spike event times during the baseline period with the memory period. Unlike the measures of association presented above, this measure is not to small numbers of SU spike events during the baseline period.

Figure 11 shows the normalized histogram of the phase at all spike events during the memory period (solid) and the baseline period (dashed). The distribution of the phases during the memory period is peaked at zero phase consistent with the coherency estimate. It is significantly different from uniform ($p < 0.01$ KS test: $N=6192$) as well as significantly different from the baseline period ($p < 0.01$ KS test: $N=6192$). This indicates that the significant memory period coherency is not due to the larger number of SU spike events during the memory period compared to the baseline period. While it is not surprising that there is a close relation between SU activity and the locally-recorded LFP, taken together these results indicate that there are coherent gamma band dynamics in neuronal activity during working memory that are not present during simple fixation.

Comparing SU and LFP activity

Comparing the power in SU and LFP activity at a particular frequency band over time and across trial condition provides more information about these processes and how they code for behavior.

Figure 12 compares SU and LFP activity in the 70 ± 20 Hz band in the preferred direction during the task. Panel a) shows line plots of the activity for the LFP (solid) and SU (dashed) at a single site. Panel b) presents the population average for LFP (solid) and SU activity (dashed). Elevations in SU activity at 70 ± 20 Hz are mirrored in the LFP throughout the task. This provides evidence that temporal structure in LFP activity is elevated during the memory period with similar dynamics to SU activity.

Figure 13 compares SU and LFP activity in the $70 \pm 20\text{Hz}$ band across saccade directions at three different epochs of the trial. Panel a) shows LFP power from a single site perisaccadically (solid), during the memory period (dashed) and baseline (dot-dashed). Panel b) shows SU power in the same frequency band from the same three periods. This shows that temporal structure in LFP activity is tuned for the preferred direction during the memory period in a similar way to SU activity recorded at the same site.

Figure 14 contains 2d plots presenting the spatiotemporal organization of SU and LFP activity. Panel a) shows SU activity at a $70 \pm 20\text{Hz}$ band from a single cell and panel b) shows LFP activity in the same frequency band at the same site. SU and LFP activity show similar organization during the task. The increase in LFP power in the $70 \pm 20\text{Hz}$ band during the memory period is significant ($p < 0.05$) in 27 of 33 (82%) of sites recorded from. The tuning of LFP power to the preferred direction during the memory period is significant ($p < 0.05$) at 28 of 33 (85%) of sites recorded from.

In addition to task-related activity in a $70 \pm 20\text{Hz}$ band there is evidence that another $20 \pm 5\text{Hz}$ frequency band of the LFP contains task-related activity. Figure 15 shows LFP power at $20 \pm 5\text{Hz}$ and compares it with $70 \pm 20\text{Hz}$ over time. Panel a) shows the 70Hz activity (solid) against the 20Hz activity (dashed) for a single site, averaged across trials in the preferred direction. Panel b) shows the same activity in a population average for one monkey. As noted before $70 \pm 20\text{Hz}$ power is elevated during working memory. Additional temporal structure in the LFP in a $20 \pm 5\text{Hz}$ band increases in power toward the end of the memory period. This is present in activity at a single site as well as in the population average and may be related to preparatory aspects of the task. The suppression of 20Hz activity peri-saccadically during saccades to all directions is also visible in activity at a single site and a population average and may be related to movement execution. These features are also present in LFP activity from the second monkey. The suppression or peri-saccadic activity compared to memory period is significant ($p < 0.05$) at 33 of 33 (100%)

sites recorded from.

SU activity is emphasized as a control signal in current work to develop a neural prosthesis but progress has been difficult because stable SU activity is hard to record using chronic cortical implants. The richness of LFP activity in multiple frequency bands, and the ease with which it can be acquired compared to SU activity, suggests that temporal structure we find in the LFP may be useful in the control of a neural prosthesis.

DISCUSSION

Elevations in SU mean firing rates define sustained memory activity but how this activity is maintained is unknown. This study investigates this issue by examining temporal structure in SU and LFP activity as well as the relation between them during working memory in area LIP of macaque parietal cortex.

We begin by discussing a methodological issue and then focus on the three principal findings of this work: i) SU activity contains temporal structure indicating the existence of dynamical memory fields; ii) SU and LFP activity are coherent in the gamma frequency band during working memory and not during simple fixation; and iii) LFP activity contains temporal structure that codes for movement planning and execution and may be useful for the control of a neural prosthesis.

General methodological issue: Time and frequency

The presence of temporal structure in neural activity is of much interest (Singer and Gray, 1995) and previous work in our lab has investigated it in these data using correlation function measures (Pezaris *et al.*, 1997a; Pezaris *et al.*, 1999). Correlation functions are often estimated in the time domain to detect temporal structure but are well known to suffer serious problems of bias and variance which are exacerbated in the context of a behaving animal (Jarvis and Mitra, 2000). Attempts to overcome these limitations when

estimating correlation functions by pooling observations across a large period of time during the experiment leads to a violation of the stationarity assumption and misinterpretation of the data (Brody, 1999).

Here we resolve significant temporal structure in neuronal activity in parietal cortex using spectral analysis. Spectral quantities are estimated in the frequency domain and while they are mathematically equivalent to correlation functions their statistical properties are better understood and better estimated. The problems of estimation bias and variance are controlled by using modern methods of multitaper spectral analysis (Thomson, 1982; Percival and Walden, 1993). Other advantages of working in the frequency domain are that i) weak non-stationarity only manifests itself in the spectrum at low frequencies; ii) nearby points in frequency are statistically independent resulting in local error bars for the estimates; and iii) the problem of the normalization of the cross-correlation function is addressed by using the coherency which is dimensionless.

In recent work, Mitra and Pesaran (1999) has applied multitaper spectral estimation to a wide range of neural data and demonstrates their advantages. In general, these are most pronounced when dealing with short segments of possibly nonstationary data. Such problems are particularly severe when studying neural activity in a behaving animal performing a structured task. Consequently, we believe the inappropriate use of time-domain correlation function measures may explain the failure of previous attempts to detect temporal structure in these data. However, if one did want to evaluate time-domain correlations, the optimal way to estimate them would be to inverse Fourier transform the corresponding spectral quantities (Pezaris *et al.*, 2000).

Understanding SU activity: Dynamical memory fields of spectral structure

An important aspect of the finding is that the spectrum of SU activity demonstrates the presence of temporal structure during working memory that comprise dynamical memory

fields. Mathematically, SU activity is a point process composed of discrete events in time (action potentials) in contrast to continuous processes such as the LFP that consist of continuous voltage changes. The simplest point process is the Poisson process which is often used to model sequences of action potentials that seem to occur randomly in time. This process is parameterized by a rate: the average number of events occurring during a given interval (Cox and Lewis, 1966). It has the important property that the events are statistically independent. This means that the probability of an event occurring in a given interval is not dependent on activity before or after the interval. The estimation of the rate parameter also reflects this because the number of events during an interval does not depend on their ordering in time. Thus, there is no temporal structure in the sequence of events in a Poisson process.

In contrast to the mean firing rate, the spectrum depends on the ordering of events in time and the process is not assumed to be random. The key difference between the spectrum of a continuous process and that of a point process is that a point process spectrum has a non-zero high frequency limit (Bartlett, 1963). If events in a process occur randomly, as for a Poisson process, the spectrum of the process is flat and uniform indicating a lack of temporal structure. A SU spectrum with significant deviations from uniformity indicates that the underlying process is not Poisson with constant rate and is therefore evidence for temporal structure in SU activity. Importantly, the mean firing rate and the spectrum for the same interval do not capture the same information. In fact, in general the estimate of the mean firing rate does not predict the frequency at the peak of the spectrum. The only property of the spectrum that the mean firing rate does characterize is the high frequency limit, or equivalently for a Poisson process, the magnitude. Our results indicate that there is broad-band temporal structure in SU activity that defines a location in space and is organized in dynamical memory fields.

The significant spectral structure we observe in SU activity has interesting consequences

for classes of the potential underlying processes. For example, the suppression at low frequencies reflects an effective refractory period for the cell of approximately 10ms. This is not related to the biophysical refractory period and represents a “2nd refractory period” during memory that may reflect a characteristic integration time for the cell. The presence of spectral suppression means that even a Poisson process with a time-varying rate cannot describe the dynamics of SU memory activity (Brillinger, 1978) and other classes of models for point process activity must be considered.

Coherent gamma band network activity during working memory

We find that during the memory period the coherency between SU and LFP activity is significant in the gamma band, 50 – 90Hz. Moreover, SUs exhibit phase locking to the LFP and preferentially fire at the peak of an LFP oscillation throughout the memory period. This temporal structure is not present during simple fixation. The result is confirmed by two controls. The first is a spike-triggered average of the extracellular potential that controls for spurious coherency due to spectral leakage of SU activity into the LFP. The second is a histogram of the phase of the LFP in the gamma band at spike times that controls for the sensitivity of the coherency estimate to small numbers of spikes during the baseline period.

The coherent structure we observe is similar to neural activity underlying the temporal code present during odor presentation in the locust (Wehr and Laurent, 1996) and provides evidence for dynamical memory fields of spectral structure that code for movement plans. The relation of SU activity to the LFP has been previously characterized in V1 of the monkey (Livingstone, 1996) and in sensorimotor cortex of macaques during exploratory and trained motor behavior (Murthy and Fetz, 1996a; Murthy and Fetz, 1996b; Donoghue *et al.*, 1998). In particular, the latter studies found relations between the processes during preparatory aspects of the task. This is possibly related to the activity we observe in the LFP in the 15 – 25Hz range, since our observations of the dynamics of spectral power in

that band are consistent with a preparatory signal.

Gamma band activity has been previously reported in the LFP of cats performing a sensorimotor task (Rouguel et al., 1979) and sustained gamma band activity has been reported in human EEG studies during a delayed-response task (Tallon-Baudry et al., 1998; Tallon-Baudry et al., 1999). These and other reports have led to the suggestion that gamma band activity may be important for cognitive processing and consciousness (Llinas et al., 1999). Investigating gamma band coherency between SUs and the LFP during working memory in a macaque may help bridge the gap between results from EEG and SU activity and offers an opportunity to study the neural substrate underlying potentially related cognitive processes in human and non-human primates (Tallon-Baudry and Bertrand, 1999). In particular, dynamical memory fields may reflect the columnar organization of cortex and could provide insight into the role of long-range reverberating circuits in the formation and sustainance of working memory activity.

LFP activity codes for movement planning and execution

The parietal cortex is implicated in movement planning, and SU activity in area LIP codes for intended eye movements and arm movements in a retinotopic coordinate frame (Andersen, 1995; Bracewell et al., 1996; Snyder et al., 1997). Recently, it has been proposed that goal-oriented retinotopic activity in parietal cortex may be useful for the control of a prosthesis (Shenoy et al., 1999). However, the difficulty of isolating activity from SUs with cortical implants could be a significant hurdle in the development of this application.

We show gamma band activity in the LFP mirrors SU activity during movement planning. Two other aspects of LFP activity are also related to the task. Firstly, the tuning of both LFP mean response and activity in the gamma band broadens peri- and post-saccadically. The significance of this is not known, but it may be related to signals to update the eye fields in area LIP following the saccade (Duhamel et al., 1992; Batista

et al., 1999). Secondly, the LFP has additional temporal structure in a distinct 15 – 25Hz frequency band with complicated dynamics that could be related to movement execution and preparatory aspects of the task. These results indicate the LFP contains a rich variety of information about the activation of parietal cortex during movement planning and execution.

Our results are evidence for coherent neuronal dynamics in SU and LFP activity during working memory organized in dynamical memory fields. The presence of significant task-related spectral structure provides evidence for a temporal structure in SU and LFP activity in parietal cortex. Since the LFP is simpler to acquire than SU activity, the presence of temporal structure in LFP activity may be useful for the control of a neural prosthesis.

Appendix

Here we present modern multitaper methods of spectral analysis used in this paper. These methods were introduced in (Thomson, 1982) and have been successfully applied to neurobiological data in recent work (Mitra and Pesaran, 1999; Prechtl et al., 1997; Cacciatore et al., 1999; Mitra et al., 1997). Multitaper methods involve the use of multiple data tapers for spectral estimation. A variety of tapers can be used, but an optimal family of orthogonal tapers is given by the prolate spheroidal functions or Slepian functions. These are parameterized by their length in time, T , and their bandwidth in frequency, W (Slepian and Pollack, 1961). For choice of T and W , up to $K = 2TW - 1$ tapers are concentrated in frequency and suitable for use in spectral estimation.

The ordinary continuous-valued time series and point processes are considered in this work form a hybrid data set and spectral analysis provides a unified framework for their analysis. For the ordinary time series consider a continuous-valued process, $x_t, t = 1, \dots, N$. The basic quantity for further analysis is the windowed Fourier transform, $\tilde{x}_k(f)$:

$$\tilde{x}_k(f) = \sum_1^N w_t(k)x_t \exp(-2\pi i f t) \quad (1)$$

$w_t(k)$ ($k = 1, 2, \dots, K$) are K orthogonal taper functions.

For the point process consider a sequence of event times $\{\tau_j\}, j = 1, \dots, N$ in the interval $[0, T]$. The quantity for further analysis of point processes is also the windowed Fourier transform, denoted by $\tilde{x}_k(f)$:

$$\tilde{x}_k(f) = \sum_{j=1}^N w_{\tau_j}(k) \exp(-2\pi i f \tau_j) - \frac{N(T)}{T} \tilde{w}_0(k) \quad (2)$$

$w_0(k)$ is the Fourier transform of the data taper at zero frequency and $N(T)$ is the total number of spikes in the interval.

When averaging over trials we introduce an additional index, i , denoting trial number, $\tilde{x}_{k,i}(f)$.

When dealing with either point or continuous processes, the multitaper estimates for the spectrum $S_x(f)$, cross-spectrum $S_{yx}(f)$ and coherency $C_{yx}(f)$ are given by

$$S_x(f) = \frac{1}{K} \sum_{k=1}^K |\tilde{x}_k(f)|^2 \quad (3)$$

$$S_{yx}(f) = \frac{1}{K} \sum_{k=1}^K \tilde{y}_k(f) \tilde{x}_k^*(f) \quad (4)$$

$$C_{yx}(f) = \frac{S_{yx}(f)}{\sqrt{S_x(f)S_y(f)}} \quad (5)$$

The auto- and cross-correlation functions can be obtained by inverse Fourier transforming the spectrum and cross-spectrum.

References

- Amit, D. (1995). The hebbian paradigm reintegrated: local reverberations as internal representation. *Behav. Brain Sci.*, 18:617–626.
- Andersen, R. (1995). Encoding of intention and spatial location in the posterior parietal cortex. *Cerebral Cortex*, 5(5):457–469.
- Baddeley, A. (1992). Working memory. *Science*, 255:556–559.
- Barash, S., Bracewell, R., Fogassi, L., Gnadt, J., and Andersen, R. (1991). Saccade-related activity in the lateral intraparietal area .1. temporal properties - comparison with area 7a. *J. Neurophysiol.*, 66:1095–1108.
- Bartlett, M. (1963). The spectral analysis of point processes. *J. R. Stat. Soc. Ser. B (Meth)*, 25:264–269.
- Batista, A., Buneo, C., Snyder, L., and Andersen, R. (1999). Reach plans in eye-centered coordinates. *Science*, 285(5425):257–260.
- Borst, A. and Theunissen, F. (1999). Information theory and neural coding. *Nature Neurosci.*, 2(11):947–957.
- Bracewell, R., Mazzonni, P., Barash, S., and Andersen, R. (1996). Motor intention activity in the macaque’s lateral intraparietal area .2. changes of motor plan. *J. Neurophysiol.*, 76:1457–1464.
- Bressler, S., Coppola, R., and Nakamura, R. (1993). Episodic multiregional cortical coherence at multiple frequencies during visual task-performance. *Nature*, 366:153–156.
- Brillinger, D. (1975). *Time series data analysis and theory*. Holt, Rinehart and Winston, Inc:New York.

- Brillinger, D. (1978). *Developments in Statistics*, volume 1, pages 33–129. Academic Press Inc.
- Brody, C. (1999). Correlations without synchrony. *Neural Comput.*, 11(7):1537–1551.
- Bruce, C. and Goldberg, M. (1985). Primate frontal eye fields. i. single neurons discharging before saccades. *J. Neurophysiol.*, 53:603–635.
- Cacciatore, T., Brodfuehrer, P., Gonzalez, J., Jiang, T., Adams, S., Tsien, R., Kristan, W., and Kleinfeld, D. (1999). Identification of neural circuits by imaging coherent electrical activity with fret-based dyes. *Neuron*, 23(3):449–459.
- Chafee, M. and Goldman-Rakic, P. (1998). Matching patterns of activity in primate prefrontal area 8a and parietal area 7ip neurons during a spatial working memory task. *J. Neurophysiol.*, 79(6):2919–2940.
- Chapin, J., Moxon, K., Markowitz, R., and Nicolelis, M. (1999). Real-time control of a robot arm using simultaneously recorded neurons in the motor cortex. *Nature Neurosci.*, 2(7):664–670.
- Cox, D. and Lewis, P. (1966). *The statistical analysis of series of events*. Chapman and Hall:London.
- deCharms, R. and Merzenich, M. (1996). Primary cortical representation of sounds by the coordination of action-potential timing. *Nature*, 381:610–613.
- Donoghue, J., Sanes, J., Hatsopoulos, N., and Gaal, G. (1998). Neural discharge and local field potential oscillations in primate motor cortex during voluntary movements. *J. Neurophysiol.*, 79(1):159–173.
- Duhamel, J., Colby, C., and Goldberg, M. (1992). The updating of the representation of visual space in parietal cortex by intended eye-movements. *Science*, 255(5040):90–92.

- Eckhorn, R., Bauer, R., Jordan, W., Brosch, M., Kruse, W., Munk, M., and Reitboeck, H. (1988). Coherent oscillations - a mechanism of feature linking in the visual cortex - multiple electrode and correlation analyses in the cat. *Biol. Cybern.*, 60(2):121–130.
- Engel, A., Konig, P., Gray, C., and Singer, W. (1990). Stimulus-dependent neuronal oscillations in cat visual-cortex - intercolumnar interaction as determined by cross-correlation analysis. *Eur. J. Neurosci.*, 2:588–606.
- Funahashi, S., Bruce, C., and Goldman-Rakic, P. (1989). Mnemonic coding of visual space in the monkey's dorsolateral prefrontal cortex. *J. Neurophysiol.*, 61:331–349.
- Fuster, J. (1995). *Memory in cerebral cortex: An empirical approach to neural networks in the human and nonhuman brain*. MIT Press:Cambridge, MA.
- Fuster, J. and Jervey, J. (1982). Neuronal firing in the inferotemporal cortex of the monkey in a visual memory task. *J. Neurosci.*, 2(3):361–375.
- Gnadt, J. and Andersen, R. (1988). Memory related motor planning activity in posterior parietal cortex of macaque. *Exp. Brain Res.*, 70:216–220.
- Goldman-Rakic, P. (1988). Topography of cognition - parallel distributed networks in primate association cortex. *Ann. Rev. Neurosci.*, 11:137–156.
- Goldman-Rakic, P. (1995). Cellular basic of working memory. *Neuron*, 14(3):477–485.
- Gray, C., Konig, P., Engel, A., and Singer, W. (1989). Oscillatory responses in cat visual-cortex exhibit inter-columnar synchronization which reflects global stimulus properties. *Nature*, 338:334–337.
- Hebb, D. (1949). *Organization of Behavior*. Wiley:New York.
- Jarvis, M. and Mitra, P. (2000). Sampling properties of the spectrum and coherency of sequences action potentials. *Neural Comput.*, Submitted.

- Kennedy, P. and Bakay, R. (1998). Restoration of neural output from a paralyzed patient by direct brain connection. *Neuroreport*, 9:1707–1711.
- Koch, K. and Fuster, J. (1989). Unit-activity in monkey parietal cortex related to haptic perception and temporary memory. *Exp. Brain Res.*, 76(2):292–306.
- Livingstone, M. (1996). Oscillatory firing and interneuronal correlations in squirrel monkey striate cortex. *J. Neurophysiol.*, 75(6):2467–2485.
- Llinas, R., Ribary, U., Contreras, D., and Pedroarena, C. (1999). The neuronal basis for consciousness. *Phil. Trans. R. Soc. Lond. Ser. B - Biol. Sci.*, 353:1841–1849.
- Lorente de No, R. (1938). *Physiology of the nervous system*, chapter Cerebral cortex architecture, intracortical connections, motor projections, pages 291–339. Oxford University Press, Oxford.
- Miller, E., Erickson, C., and Desimone, R. (1996). Neural mechanisms of visual working memory in prefrontal cortex of the macaque. *J. Neurosci.*, 16:5154–5167.
- Mitra, P., Ogawa, S., Hu, X., and Ugurbil, K. (1997). The nature of spatiotemporal changes in cerebral hemodynamics as manifested in functional magnetic resonance imaging. *Mag. Res. Med.*, 37:511–518.
- Mitra, P. and Pesaran, B. (1999). Analysis of dynamic brain imaging data. *Biophys. J.*, 76:691–708.
- Miyashita, Y. and Chang, H. (1988). Neuronal correlate of pictorial short-term memory in the primate temporal cortex. *Nature*, 331:68–70.
- Murthy, V. and Fetz, E. (1996a). Oscillatory activity in sensorimotor cortex of awake monkeys: Synchronization of local field potentials and relation to behavior. *J. Neurophysiol.*, 76(6):3949–3967.

- Murthy, V. and Fetz, E. (1996b). Synchronization of neurons during local field potential oscillations in sensorimotor cortex of awake monkeys. *J. Neurophysiol.*, 76(6):3968–3982.
- Percival, D. and Walden, A. (1993). *Spectral analysis for physical applications*. Cambridge University Press, Cambridge, UK.
- Pezaris, J. (2000). *Local circuitry in LIP*. PhD thesis, California Institute of Technology.
- Pezaris, J., Sahani, M., and Andersen, R. (1997a). Extracellular recording from adjacent neurons: Ii. correlations in macaque parietal cortex. In *Soc. Neurosci. Abs.*, volume 23.
- Pezaris, J., Sahani, M., and Andersen, R. (1997b). Tetrodes for monkeys. In Bower, J., editor, *Computational Neuroscience*. Plenum Press:New York.
- Pezaris, J., Sahani, M., and Andersen, R. (1999). Response-locked changes in auto- and cross-covariations in parietal cortex. *Neurocomp.*, 26-27:471–476.
- Pezaris, J., Sahani, M., and Andersen, R. (2000). Spike train coherence in macaque parietal cortex during a memory saccade task. *Neurocomp.*, In press.
- Prechtl, J., Cohen, L., Pesaran, B., Mitra, P., and Kleinfeld, D. (1997). Visual stimuli induce waves of electrical activity in turtle cortex. *Proc. Natl. Acad. Sci. USA*, 94(14):7621–7626.
- Rao, C. (1965). *Linear Statistical Inference and its Applications*. Wiley:New York.
- Reece, M. and O’Keefe, J. (1989). The tetrode: An improved technique for multi-unit extracellular recording. In *Soc. Neurosci. Abs.*, volume 15.
- Roelfsema, P., Engel, A., Konig, P., and Singer, W. (1997). Visuomotor integration is associated with zero time-lag synchronization among cortical areas. *Nature*, 385(6612):157–161.

- Rosenberg, J., Amjad, A., Breeze, P., Brillinger, D., and Halliday, D. (1989). The fourier approach to the identification of functional coupling between neuronal spike trains. *Prog. Biophys. Molec. Biol.*, 53:1–31.
- Rougel, A., Bouyer, J., Dedet, L., and Debray, O. (1979). Fast somato-parietal rhythms during combined focal attention and immobility in baboon and squirrel monkey. *Electro. Clin. Neurophysiol.*, 46:310–319.
- Sahani, M. (1999). *Latent variable models for neural data analysis*. PhD thesis, California Institute of Technology.
- Sahani, M., Pezaris, J., and Andersen, R. (1998). On the separation of signals from neighboring cells in tetrode recordings. In Jordan, M., Kearns, M., and Solla, S., editors, *Advances in Neural Information Processing Systems 10*. MIT Press:Cambridge, MA.
- Sakata, H., Taira, M., Murata, A., and Mine, S. (1995). Neural mechanisms for the visual guidance of hand action in the parietal cortex of the monkey. *Cereb. Cortex.*, 5:429–438.
- Sanes, J. and Donoghue, J. (1993). Oscillations in local-field potentials of the primate motor cortex during voluntary movement. *Proc. Natl. Acad. Sci. USA*, 90:4470–4474.
- Seung, H. (1996). How the brain keeps the eyes still. *Proc. Natl. Acad. Sci. USA*, 93:13339–13344.
- Shenoy, K., Kureshi, S., Meeker, D., Gillikin, B., Batista, A., Buneo, C., Cao, S., Burdick, J., and Andersen, R. (1999). Toward prosthetic systems controlled by parietal cortex. In *Soc. Neurosci. Abs.*, volume 25.
- Singer, W. and Gray, C. (1995). Visual feature integration and the temporal correlation hypothesis. *Ann. Rev. Neurosci.*, 18:555–586.

- Slepian, D. and Pollack, H. (1961). Prolate spheroidal wavefunctions. fourier analysis and uncertainty i. *Bell Sys. Tech. J.*, 40:43–63.
- Snyder, L., Batista, A., and Andersen, R. (1997). Coding of intention in the posterior parietal cortex. *Nature*, 386(6621):167–170.
- Tallon-Baudry, C. and Bertrand, O. (1999). Oscillatory gamma activity in humans and its role in object representation. *Trends Cog. Sci.*, 3(4):151–162.
- Tallon-Baudry, C., Bertrand, O., Peronnet, F., and Pernier, J. (1998). Induced gamma-band activity during the delay of a visual short-term memory task in humans. *J. Neurosci.*, 18(11):4244–4254.
- Tallon-Baudry, C., Kreiter, A., and Bertrand, O. (1999). Sustained and transient oscillatory responses in the gamma and beta bands in a visual short-term memory task in humans. *Vis. Neurosci.*, 16(3):449–459.
- Thomson, D. (1982). Spectrum estimation and harmonic analysis. *Proc. IEEE*, 70:1055–1096.
- Thomson, D. (1994). Projection filters for data analysis. In *Proc. Seventh IEEE SP Work. Stat. Sig. and Array Proc.*, pages 39–42, Quebec, Canada.
- Thomson, D. J. and Chave, A. D. (1991). *Advances in Spectrum Analysis and Array Processing*, volume 1, pages 58–113. Prentice Hall.
- Ueda, N. and Nakano, R. (1994). Mixture density estimation via em algorithm with deterministic annealing. *Proc. IEEE: Neural networks and signal processing*, 69:69–77.
- Wang, X.-J. (1999). Synaptic basis of cortical persistent activity: the importance of nmda receptors to working memory. *J. Neurosci.*, 19:9587–9603.

Wehr, M. and Laurent, G. (1996). Odour encoding by temporal sequences of firing in oscillating neural assemblies. *Nature*, 384:162–166.

Zhou, Y. and Fuster, J. (1996). Mnemonic neuronal activity in somatosensory cortex. *Proc. Natl. Acad. Sci. USA*, 93(19):10533–10537.

Figure Captions

Figure 1. The memory-saccade task The monkey performs a memory-saccade to one of eight saccade directions. a) The trial begins with the illumination of a fixation light at the center of the screen. The monkey saccades to the fixation light, to which the monkey maintains fixation for one second, which determines the baseline period. b) A target is then flashed in one of eight points for 100ms and extinguished. c) The monkey must maintain fixation for a further second at which point d) the fixation light is extinguished and the monkey performs a saccade to the remembered target location. When the saccade is completed and the monkey's eye position is within 2° of the target, e) it reilluminates and the monkey is rewarded with a drop of juice. A corrective minisaccade follows the target reillumination. There is a short intertrial interval before the fixation light reilluminates signalling the start of a new trial.

Figure 2. Sample data a) One channel of raw tetrode data sampled at 20kHz shown for a memory-saccade trial during a saccade to the preferred direction. The saccade was down and to the left and (x,y) eye position traces are shown beneath. Behavioral events are indicated below eye position traces establishing the convention to be used in later figures. Dotted lines indicated the illumination of the fixation light. Solid lines indicate illumination of the target. The points indicate saccades. When available, color is used in place of symbols. Blue indicates illumination of the fixation light, red indicates illumination of the target and green marks the saccade. These raw traces were high-pass filtered and thresholded to determine spike event times. These events were then classified to give point processes of single unit activity. Note increased activity during the memory period. b) The data in panel a) viewed on an expanded time base from 0.2–0.5s. Broad-band low frequency ($< 100\text{Hz}$) and SU spiking activity are visible. The amplitude of spikes from SU activity is not large compared to the amplitude of the broad-band activity.

Figure 3. SU activity The PSTH is shown for a single unit recorded during the memory saccade task as a function of saccade direction. A strong increase in single cell activity during the memory period is seen for saccades to the left. This defines the preferred direction of the cell. Eye position traces, x and y coordinates, for each trial are shown beneath each panel. Behavioral events during the trial are shown beneath each histogram according to the convention described for Figure 2. Spike rasters are shown for each trial at the top of each panel.

Figure 4. SU and LFP mean response Line and 2d plots showing the mean response of SU and LFP activity averaged across saccades in each direction.

a) 2d plot of the SU PSTH (as seen in figure 3) averaged across trials aligned to the initial target onset as a function of saccade direction. Time is on the x-axis and saccade direction, aligned with 0 degrees the preferred direction, is on the y-axis. b) Line plots of SU mean response in panel a) in preferred (solid) and anti-preferred (dashed) directions. c) 2d plot of the LFP mean response averaged across trials aligned to the initial target onset as a function of saccade direction. Time is on the x-axis and saccade direction, aligned with 0 degrees the preferred direction, is on the y-axis. d) Line plot of the LFP mean response in the preferred (solid) and anti-preferred (dashed) directions.

SU and LFP mean responses contain tuned activity. The LFP mean response also contains tuned low frequency postsaccadic activity following saccades made to all directions.

Figure 5. Spectral structure in SU activity Line and 2d plots showing the spectrum of SU activity in the preferred direction.

a) Line plots of the spectrum during the memory (red) and baseline (blue) period for a single cell. Solid lines indicate the trial-average spectrum. Dashed lines indicate 95% error bars estimated using the jackknife. Dotted lines indicate the high-frequency limit. b) 2d plot of

the spectrogram for a single cell with time on the x-axis and frequency on the y-axis. Power is color-coded on a log scale. Behavioral events are indicated below. c) Line plots of the population average spectrum during the memory (red) and baseline (blue) period for one monkey. Solid lines indicate the spectrum and dotted lines indicate the high-frequency limit. d) 2d plot of the population average spectrogram with time on the x-axis and frequency on the y-axis. Power is color-coded on a log scale. Behavioral events are indicated below.

Significant spectral structure is present during the memory period and not during the baseline period. During the memory period a significant peak in the spectrum is present above 30Hz and significant suppression of the spectrum is present below 20Hz for a single cell and in the population averages. This means that SU activity cannot be well modelled as a rate-varying, inhomogeneous Poisson process. Spectrograms show that the spectral structure is present from the initial target onset through the saccade.

Figure 6. Spectral structure in LFP activity Line plots showing the spectrum of LFP activity during the memory and baseline periods in the preferred and anti-preferred directions.

a) Memory (solid) and baseline (dashed) activity at a single site during saccades to the preferred direction. b) Memory activity at a single site during saccades to the preferred (solid) and anti-preferred (dashed) direction. c) Population average memory (solid) and baseline (dashed) activity during saccades to the preferred direction. d) Population average memory activity during saccades to the preferred (solid) and anti-preferred (dashed) direction.

Gamma band activity is elevated in the memory period for the preferred direction at a single site and in the population average. The narrow peak in a recording from a single site is broadened in the population average.

Figure 7. Spectral structure in LFP activity Spectrograms of LFP activity averaged

across trials during saccades to the preferred and anti-preferred direction. Time is on the horizontal axis and frequency is on the vertical axis. Spectra are color-coded on a log scale.

a) Activity from a single site in the preferred direction. b) Activity from a single site in the anti-preferred direction. c) Population average activity in the preferred direction from one monkey. d) Population average activity in the anti-preferred direction from one monkey.

A strong increase in gamma band 50–90Hz activity localized to the memory period is present during saccades to the preferred direction in a single site and the population average. This is not seen in activity in the anti-preferred direction.

Figure 8. SU - LFP coherency Coherency between SU and LFP activity at a single site in the preferred direction.

Time is on the horizontal axis and frequency on the vertical axis. Coherence is color-coded on a linear scale. The phase of the coherency is indicated by an arrow at each frequency that the coherence is significant ($p < 0.01$). The mean firing rate of the SU activity and rasters showing the trial-by-trial activity are displayed above. Eye movement traces and behavioral events are shown below.

Coherence is only significant during the memory period in the gamma frequency band, 40–90Hz.

Figure 9. SU - LFP population coherency Population average coherency of SU and LFP activity in the preferred direction from one monkey. Time is on the horizontal axis and frequency on the vertical axis. The coherence is color-coded on a linear scale. The phase of the coherency is indicated by an arrow at each frequency where the coherence is significant ($p < 0.01$). Behavioral events are shown below. The significant increase in single site coherence during the memory period is also present in the population average. This indicates that the phase of the coherency is constant across different recordings in area LIP.

Figure 10. Spike-triggered potential Spike-triggered average potential for activity from a single cell at a single site during trials for saccades to the preferred direction. Baseline activity and memory period activity were averaged separately.

a) Spike-triggered average potential for SU activity during the baseline period. b) Spike-triggered average potential during the memory period

During the baseline period structure is present before the spike indicating weak locking to the extracellular potential in the generation of a spike. Memory period activity shows oscillatory structure centered on the spike event time indicating locking to temporal structure in the extracellular potential.

Figure 11. Phase histogram The distribution of the phase of the $70 \pm 20\text{Hz}$ activity in the LFP at the spike event times for all cells in the data set during saccades to their preferred direction. Memory (solid) and baseline (dashed) period distributions are compared. Strong locking to the $70 \pm 20\text{Hz}$ field potential oscillation at zero phase lag is present during the memory period and not during the baseline period.

Figure 12. Dynamics of 70Hz power in SU and LFP activity The dynamics of the power of neuronal activity in the $70 \pm 20\text{Hz}$ gamma frequency band

a) LFP (solid) and SU (dashed) gamma band activity at a from a single cell at a single site. b) Population average of LFP (solid) and SU (dashed) activity in one monkey.

Dynamics of SU and LFP gamma band activity are very similar in all phases of the trial.

Figure 13. Tuning of 70Hz power in SU and LFP activity Tuning of the power of neuronal activity in the $70 \pm 20\text{Hz}$ gamma frequency band at a single site.

a) Baseline (dot-dash) memory (solid) and perisaccadic (dashed) SU activity at 70Hz is shown against saccade direction. The preferred direction aligned to the center of the plot.

b) Baseline (dot-dash) memory (solid) and perisaccadic (dashed) LFP activity at 70Hz is shown against saccade direction. The preferred direction aligned to the center of the plot.

Tuning of SU and LFP gamma band memory period activity are very similar. Memory and perisaccadic activity are tuned while the baseline period shows no tuned activity.

Figure 14. SU and LFP 70Hz power Power in SU and LFP activity in the $70 \pm 20\text{Hz}$ frequency band averaged across trials for saccades to different directions.

a) 2d plot of SU activity from a single cell. Power is color-coded on a linear scale. Time is on the horizontal axis. Saccade direction is on the vertical axis. The preferred direction is aligned to 0 degrees. Behavioral events are shown below. b) 2d plot of LFP activity from a single site shown in the same way as SU activity in panel a).

Figure 15. LFP power at 20Hz and 70Hz The LFP activity is compared between frequency bands at $70 \pm 20\text{Hz}$ and $20 \pm 5\text{Hz}$ for trials with saccades to the preferred directions.

a) LFP activity at 70Hz (solid) and 20Hz (dashed) from a single site. b) Population average LFP activity at 70Hz (solid) and 20Hz (dashed) from one monkey.

70Hz activity is elevated from the initial target onset through the saccade. 20Hz activity rises toward the end of the memory period and is suppressed peri-saccadically. The elevated 70Hz activity may be related to movement planning. The suppression in 20Hz activity peri-saccadically may be related to movement execution. The rise in 20Hz activity toward the end of the memory period may reflect preparatory aspects of the task.

Figure 1

Figure 1

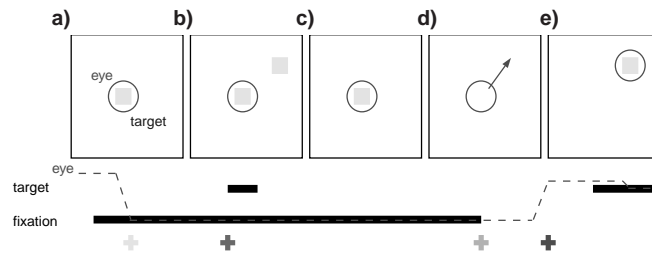


Figure 2

Blank Figure.
See attached .jpg file.

Figure 3

Blank Figure.
See attached .jpg file.

Figure 4

Blank Figure.
See attached .jpg file.

Figure 5

Blank Figure.
See attached .jpg file.

Figure 6

Figure 6

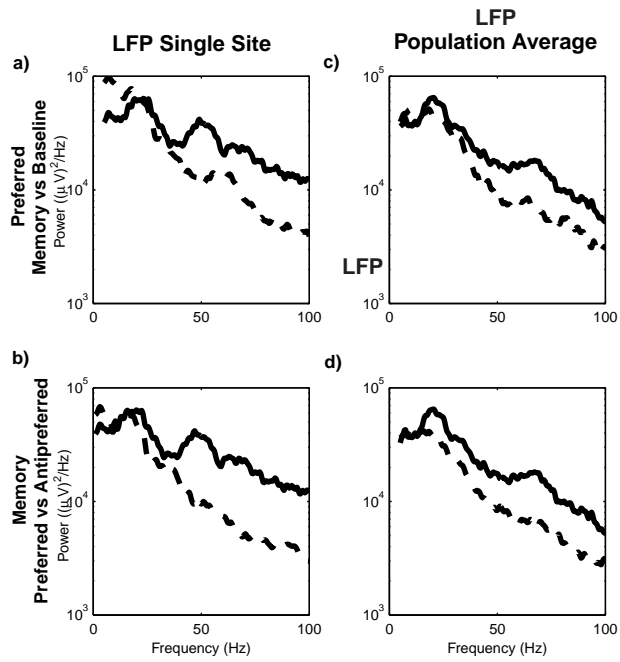


Figure 7

Blank Figure.
See attached .jpg file.

Figure 8

Blank Figure.
See attached .jpg file.

Figure 9

Figure 9

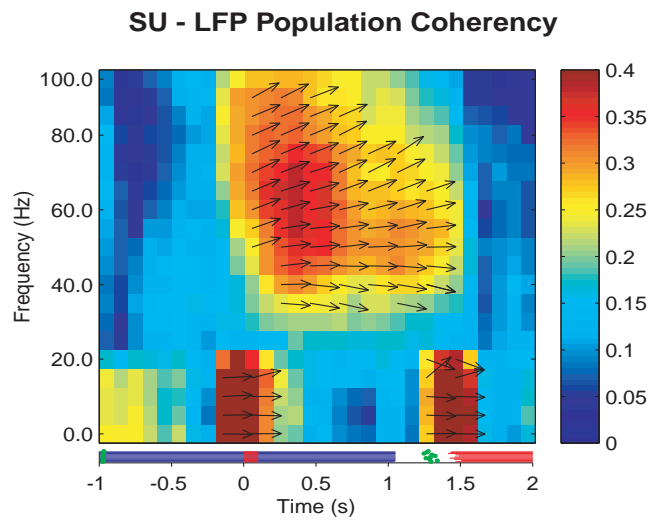


Figure 10

Blank Figure.
See attached .jpg file.

Figure 11

Figure 11

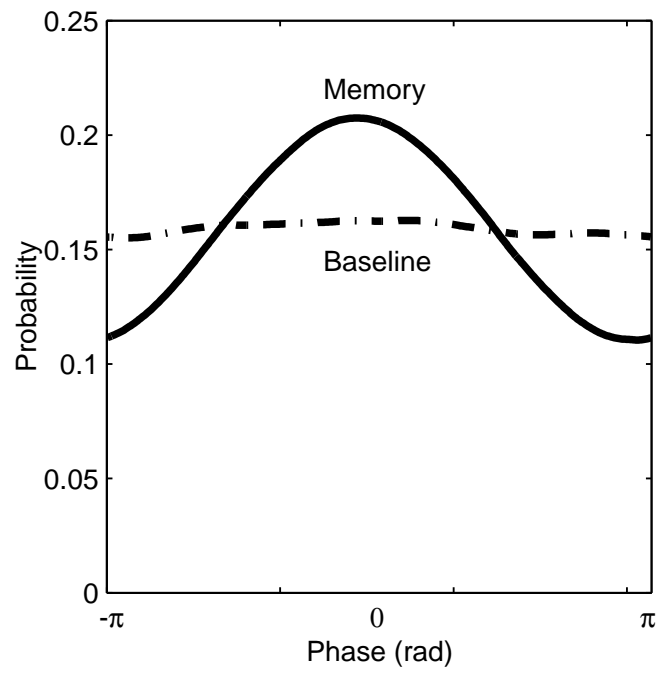


Figure 12

Figure 12

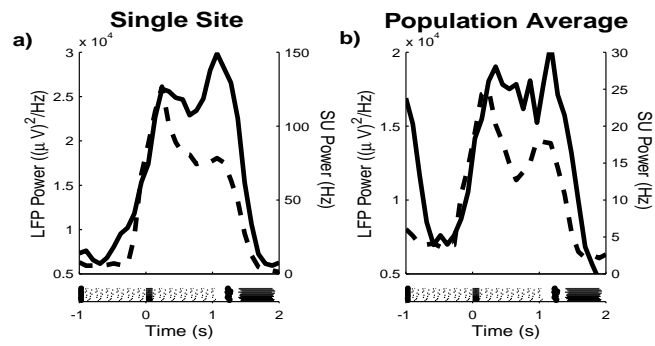


Figure 13

Figure 13

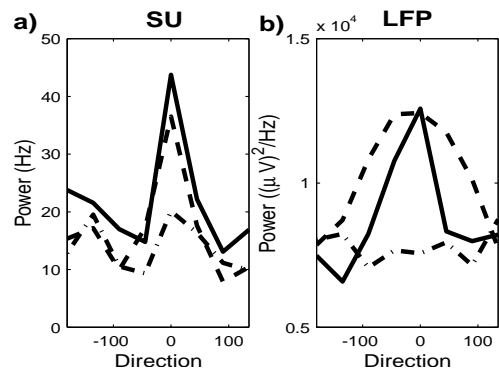


Figure 14

Figure 14

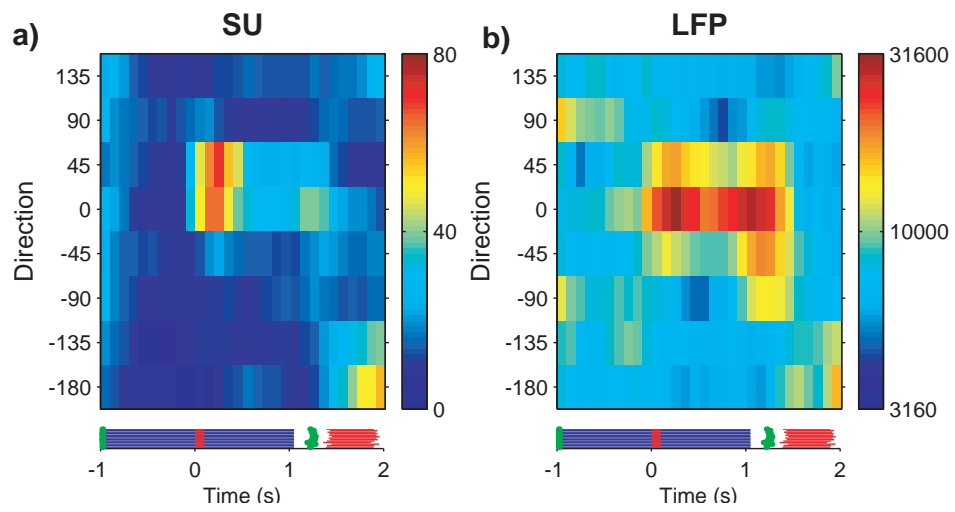
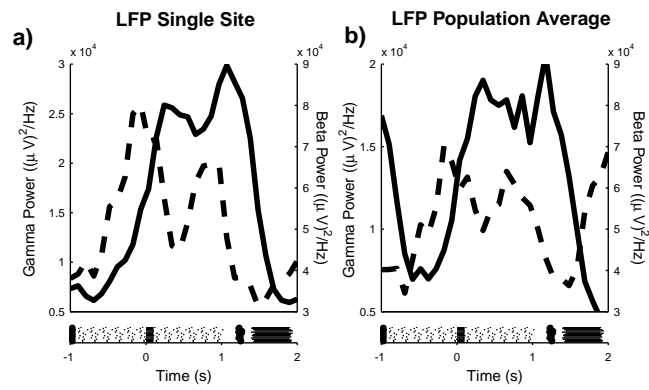


Figure 15

Figure 15



This figure "Coherency_1.jpg" is available in "jpg" format from:

<http://arxiv.org/ps/q-bio/0309034v1>

This figure "LFPSpectra_1.jpg" is available in "jpg" format from:

<http://arxiv.org/ps/q-bio/0309034v1>

This figure "Mean.jpg" is available in "jpg" format from:

<http://arxiv.org/ps/q-bio/0309034v1>

This figure "PSTH.jpg" is available in "jpg" format from:

<http://arxiv.org/ps/q-bio/0309034v1>

This figure "RawData.jpg" is available in "jpg" format from:

<http://arxiv.org/ps/q-bio/0309034v1>

This figure "STA.jpg" is available in "jpg" format from:

<http://arxiv.org/ps/q-bio/0309034v1>

This figure "SpikeSpectra.jpg" is available in "jpg" format from:

<http://arxiv.org/ps/q-bio/0309034v1>